Electronic Supplemental Information (ESI)

Broadscale Resolving Power Performance of a High Precision Uniform Field Ion Mobility-Mass Spectrometer

Jody C. May,[a] James N. Dodds,[a] Ruwan T. Kurulugama,[b] George C. Stafford,[b] John C. Fjeldsted,[b] and John A. McLean [a]*

[a] Department of Chemistry; Center for Innovative Technology; Vanderbilt Institute for Integrative Biosystems Research and Education; Vanderbilt Institute of Chemical Biology; Vanderbilt University, Nashville, TN

[b] Agilent Technologies, Santa Clara, CA

*Corresponding Author. Email: john.a.mclean@vanderbilt.edu

Correlation of theoretical drift time to experimental measurements

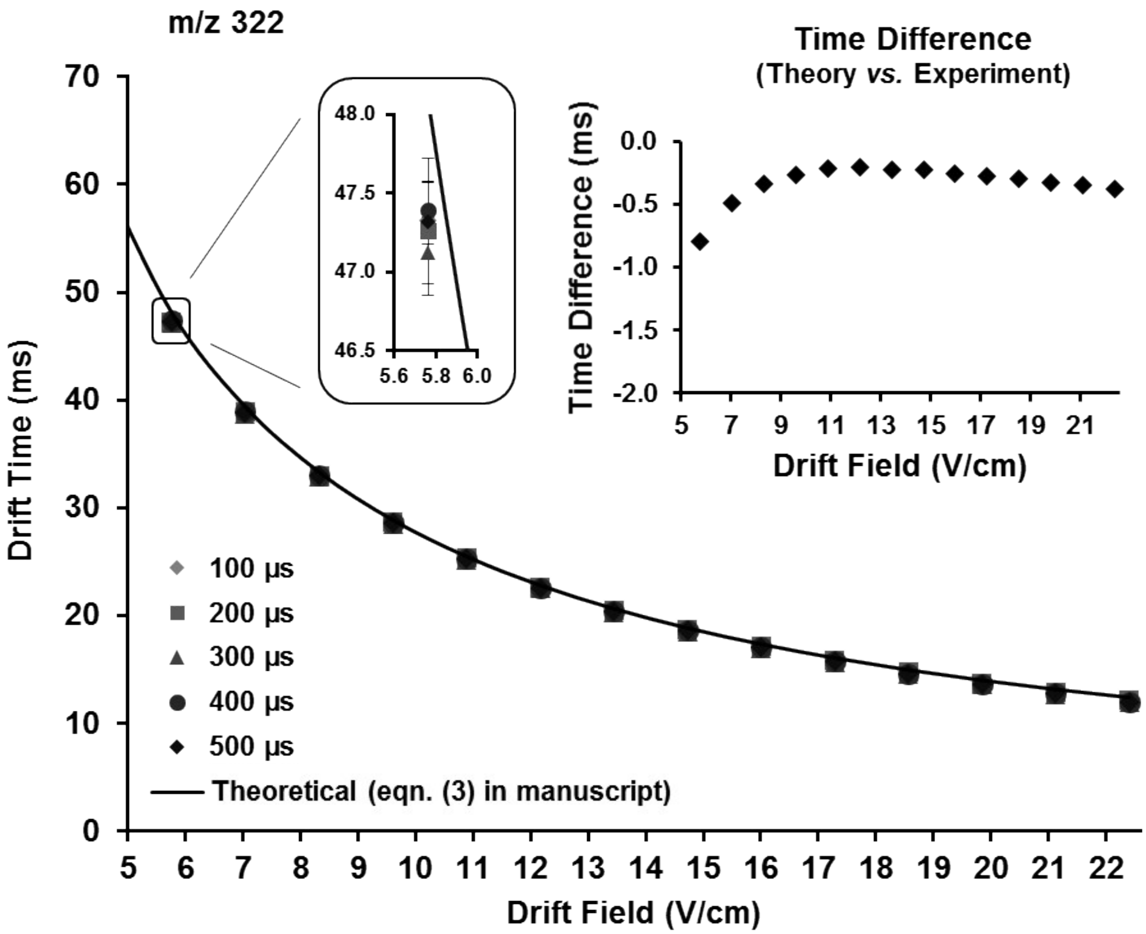

Figure S1. Correlation of theoretical drift time values obtained from eqn. (3) (in manuscript) to experimental drift times for the m/z 322 ion. Each point represents 4 replicate measurements. For drift time, theory accurately predicts the experimental results. The expanded region at low drift field where error is highest (left inset) illustrates that the gate width contribution is within experimental error. The right inset demonstrates the difference between experimental and theoretical drift times, while not zero, is systematically reproducible at the higher drift fields (beyond 8 V/cm). The higher error at low drift field is reproducible for the other ions and we infer that this represents error associated with the extrapolation procedure used to correct the drift time for the non-mobility component. Note here that in order to utilize the IMS drift length (78.1 cm) in eqn. (3), the experimental drift times are corrected by subtracting the non-mobility time component, as obtained by conducting the stepped drift field linear regression analysis used in determining ion transport data [1]. The low drift field values (below 8 V/cm) are not utilized in this linear regression analysis.

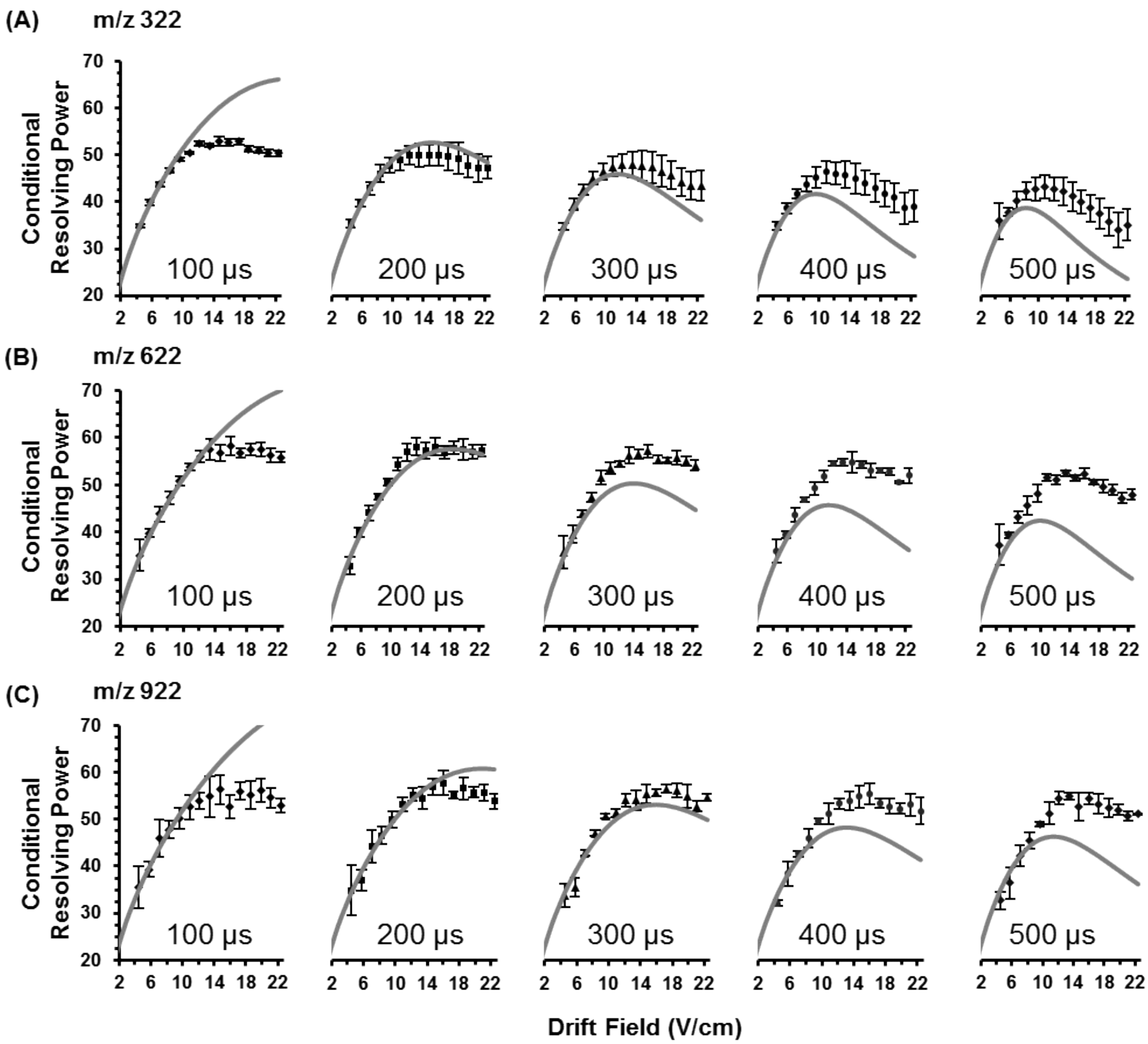

Figure S2. Comparison of the conditional resolving power theory (eqn. (5) in manuscript, solid lines) with empirical results for each of the five gate widths investigated, for (A) m/z 322, (B) m/z 622, and (C) m/z 922. While conditional resolving power predicts the qualitative shape of the resolving power curves, a notable deviation is observed between experiment and theory for high and low gate widths, with the most favorable correlation occurring at *ca.* 200 µs (second plot in each panel).

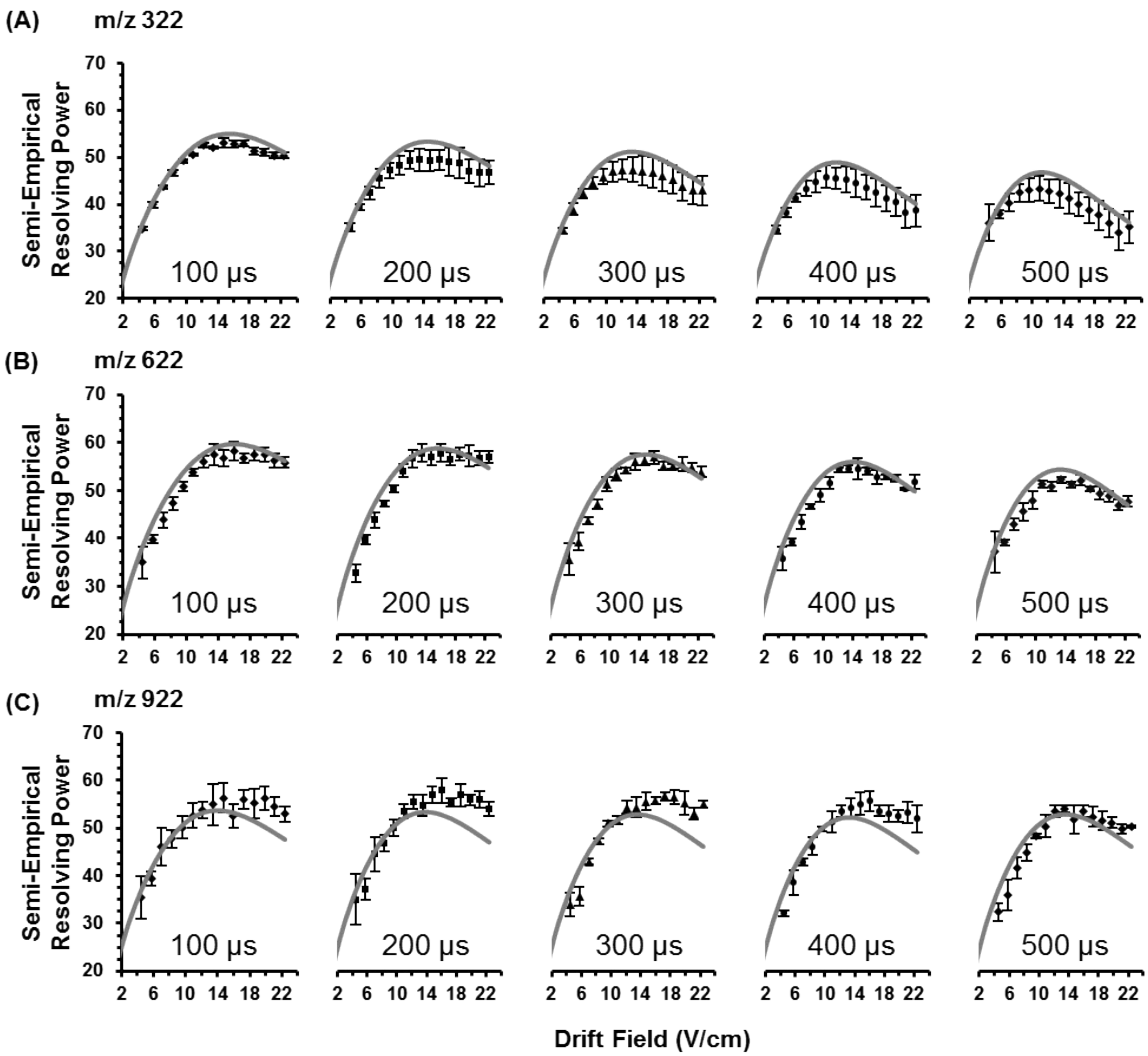

Figure S3. Comparison of the semi-empirical resolving power theory (eqn. (7) in manuscript) to experimental results using the coefficients determined for the current instrumentation used in this study. Empirical results are the same as shown in Fig. S2. Good quantitative correlation is observed for these three ions across all gate widths investigated.

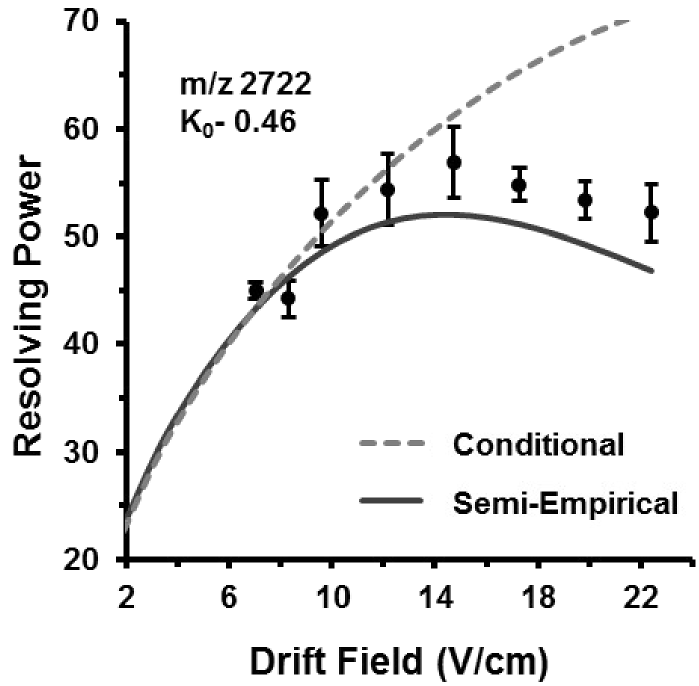

Figure S4. Comparison of the conditional resolving power formula with the derived semi-empirical method for a low mobility ion (ATM m/z 2722) at an applied gate width of 200 µs. Conditional resolving power theory significantly over-predicts the resolving power at this low mobility, which is consistent with the trend observed for the other ATM ions (Fig. S2). Semi-empirical resolving power is closer to experimental measurements, with a slight under-prediction of the resolving power, which is similar to the correlation observed for the m/z 922 system (Fig. S3).

Details of the procedure for determining the semi-empirical coefficients

The procedure used in this work to derive the semi-empirical coefficients is based on the same linear regression analysis first outlined by Siems *et al.* [2], but differs slightly in how the coefficients are determined from the least-squares fitting. The expression for peak width derived from first-principles kinetic theory by Revercomb and Mason (eqn. (4) in manuscript) [3] is as follows:

$$\Delta t = \left({t_g}^2 + \frac{16ln2 \cdot k_B T}{V \cdot z \cdot e} \cdot {t_d}^2 \right)^{\frac{1}{2}} \tag{S1}$$

The semi-empirical resolving power expression introduces three additional terms to eqn. (S1):

$$\Delta t = \left(\gamma + \beta \cdot {t_g}^2 + \alpha \cdot \frac{T}{V} \cdot {t_d}^2 \right)^{\frac{1}{2}} \tag{S2}$$

Where the "α" and "β" coefficients are multiplers to the diffusion and gate width terms, respectively, and the "γ" coefficient is introduced as an added source of variance within the square root. Comparing the diffusion term on the RHS of eqn. (S1) to eqn. (S2), we obtain the following correspondence to "α":

$$\alpha = \frac{16ln2 \cdot k_B}{z \cdot e} \tag{S3}$$

Which for singly-charged ions ($z = 1$) gives the "ideal" value of $\alpha = 0.957 \times 10^3$ V/K. Likewise, "ideal" values for the other coefficients are $\beta = 1$ and $\gamma = 0$ s^2.

Determination of the "α" coefficient

Equation S1 can be rearranged to yield the following expression:

$$\Delta t^2 = \alpha \cdot \left(\frac{T}{V} \cdot {t_d}^2 \right) + \left(\beta \cdot {t_g}^2 + \gamma \right) \tag{S4}$$

The "α" coefficient is then determined by plotting the square of the experimental peak width (Δt^2) as a function of the diffusion term ($\frac{T}{V} \cdot {t_d}^2$). A slope-intercept analysis of the least-squares linear fit to the data is then used to obtain the following for the slope (m):

$$m = \alpha \tag{S5}$$

and the y-intercept (y_0):

$$y_0 = \beta \cdot {t_d}^2 + \gamma \tag{S6}$$

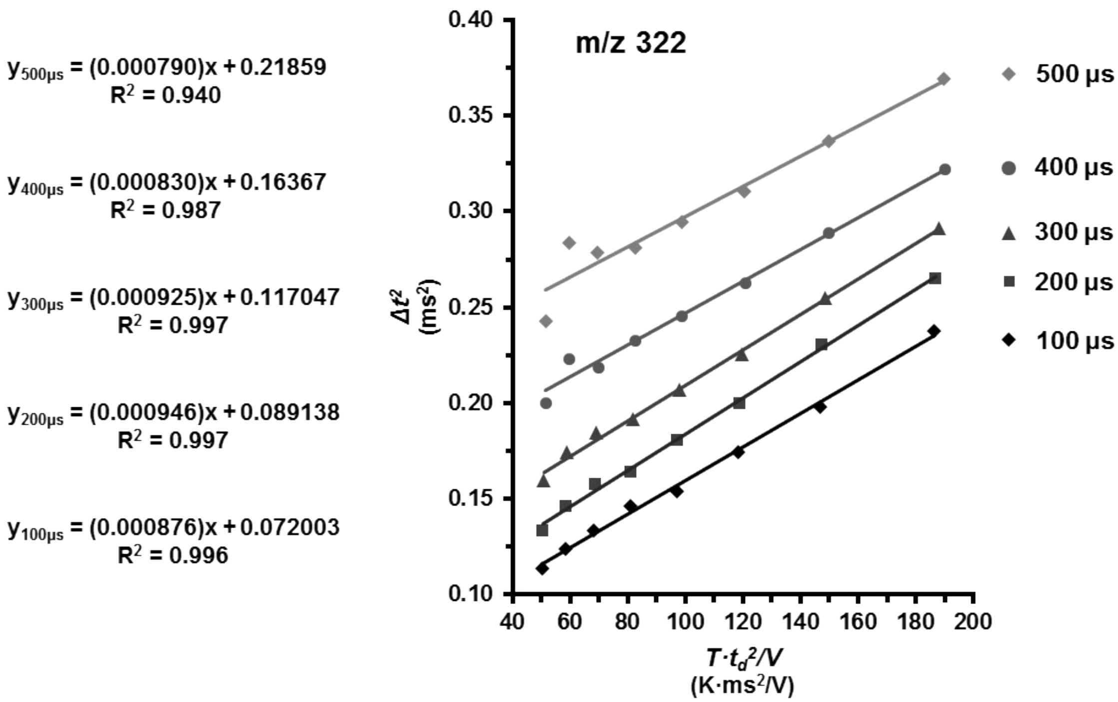

Figure S5. Linear regression analysis used to determine the "α" coefficient, shown here for the m/z 322 ion. Each line represents a different dataset obtained using one of five different initial ion gate widths (100, 200, 300, 400, and 500 µs); data within each gate width is measured for eight separate drift fields (13.4, 14.7, 16.0, 17.3, 18.6, 19.9, 21.1, and 22.4 V/cm). Note that this analysis was conducted for nine components of the ATM solution (m/z 322, 622, 922, 1222, 1522, 1822, 2122, 2422, and 2722) and the slopes obtained from each linear fit was averaged to obtain the "α" used in the manuscript.

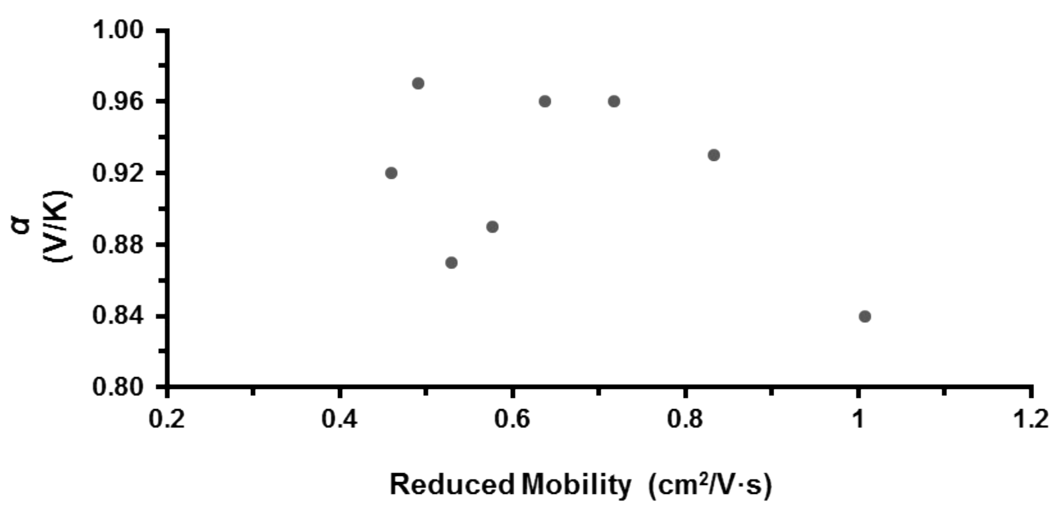

Figure S6. Variation of all "α" values obtained from eight different ions as a function of the ion's reduced mobility value (K_0). No strong correlation between "α" and K_0 was observed, and so the average "α" (0.000910 ± 0.00005 V/K) was utilized in all subsequent analysis.

Determination of the "β" coefficient

As was done previously, eqn. (S1) can be rearranged to yield the following expression:

$$\Delta t^2 = \beta \cdot \left(t_g{}^2\right) + \left(\alpha \cdot \frac{T}{V} \cdot t_d{}^2 + \gamma\right) \tag{S7}$$

The "β" coefficient is determined here by plotting the square of the experimental peak width (Δt^2) as a function of the square of the gate width ($t_g{}^2$). A slope-intercept analysis of the least-squares linear fit to the data is then used to obtain the following for the slope (m):

$$m = \beta \tag{S8}$$

and the y-intercept (y_0):

$$y_0 = \cdot \alpha \cdot \frac{T}{V} \cdot t_d{}^2 + \gamma \tag{S9}$$

The slope corresponding to the highest field (22.4 V/cm) is used as the "β" coefficient in subsequent analyses as this represents the situation in which ions spend the least amount of time in the drift tube, and thus would exhibit the strongest "memory" of the initial gating event.

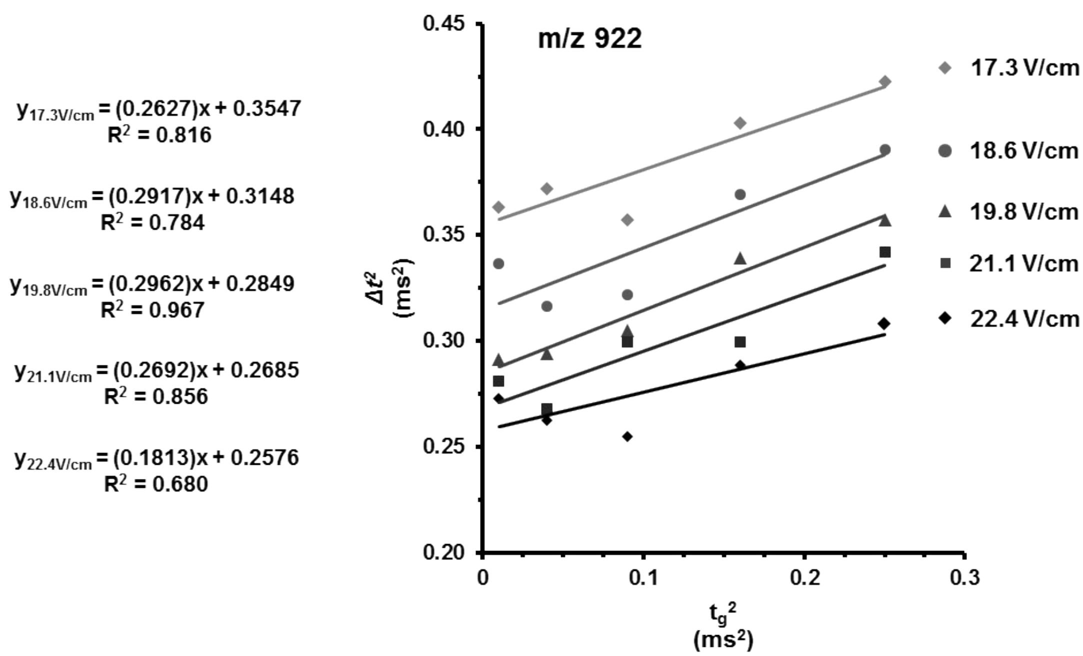

Figure S7. Linear regression analysis used to determine the "β" coefficient, shown here for the m/z 922 ion. A best fit line was plotted for data from each of five field strengths (17.3, 18.6, 19.8, 21.1, and 22.4

V/cm) with each data set representing measurements obtained from the five gate widths evaluated (100, 200, 300, 400, and 500 μs). While additional data was obtained at lower drift fields, the higher fields represent conditions in which ions transit the drift region faster and thus would retain more memory of the influence of the initial gating event. This also introduces some additional variability in the data, as noted by the inconsistent slope at the highest field investigated (22.4 V/cm).

Determination of the "γ" coefficient

The determination of "γ" described here deviates slightly from the original work by Siems *et al*. In the original work, "γ" was determined by performing a linear regression analysis on all y-intercept values obtained from the "α" and "β" plots to generate new datasets which represent hypothetical data in the limits of zero gate width, and infinite voltage, respectively. The y-intercepts obtained from these hypothetical datasets is "γ" [2]

Here, we utilize the values obtained for "α" and "β" directly into the y-intercept expressions (eqn. (S6) and eqn. (S9) and solve for "γ" directly for each linear fit. This results in a tabulated set of "γ" values for each ion investigated. To obtain "γ" from the "α" expression *via.* eqn. (S6), the "β" obtained at the highest drift field is utilized, which represents the case where ions spend the least amount of time in the drift region. This also simplifies the analysis since only a single "α" value is evaluated for each data series. Obtaining "γ" from the "β" expression *via.* eqn. (S9) is more straightforward and involves solving for "β" by utilizing the average "α" obtained for each ion. The average is rationalized here since "α" does not exhibit a strong dependence on the specific ion utilized in the analysis (Fig. S6).

Mobility dependence on the "β" and "γ" coefficients

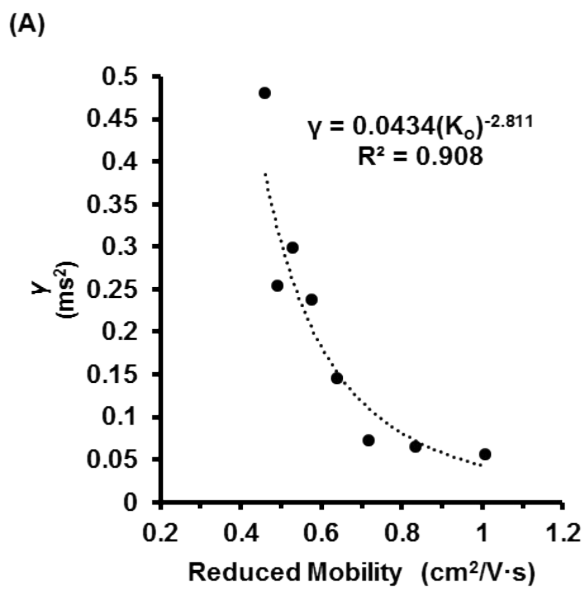

Figure S8. Regression analysis used to determine the function which relates the semi-empirical coefficients (β and γ) to the ion's reduced mobility, K_0. (A) The curve best fitting the data is a power fit based on eight high mass ions in the ATM solution (m/z 622, 922, 1222, 1522, 1822, 2122, 2422, and 2722). (B) Fitting parameters for the "β" term as a function of mobility for the m/z 322, 622, and 922 ions. These equations are reintroduced into the semi-empirical resolving power expression (eqn. (7) in the manuscript) in order to introduce the ion-specific contribution to each of these terms.

Semi-empirical resolving power expression

Using the coefficients and coefficient expressions summarized in Table 1 in the manuscript, the semi-empirical resolving power equation is expanded to the following functional form:

$$R_{SE} = \frac{\frac{L}{K_0 \cdot E_0} \cdot \left(\frac{273.15}{T} \cdot \frac{P}{760}\right) \cdot 1000}{\left[(0.0434 \cdot K_0{}^{-2.811}) + (0.3145 \cdot K_0{}^2 - 0.035 \cdot K_0) \cdot t_g{}^2 + (0.00091) \cdot \frac{T}{V} \cdot \left(\frac{L}{K_0 \cdot E_0} \cdot \left(\frac{273.15}{T} \cdot \frac{P}{760}\right) \cdot 1 \right.\right.\right.} \quad \text{(S10)}$$

The 10^3 multipliers in the numerator and the RHS of the denominator within the square root term is necessary to convert drift time to milliseconds, which is the unit used in the semi-empirical expressions. Note also that the gate time (t_g) term is in milliseconds (whereas conventionally this is reported in microseconds).

References

[1] May, JC; Goodwin, CR; Lareau, NM; Leaptrot, KL; Morris, CB; Kurulugama, RT; Mordehai, A; Klein, C; Barry, W; Darland, E; Overney, G; Imatani, K; Stafford, GC; Fjeldsted, JC; McLean, JA; “Conformational Ordering of Biomolecules in the Gas Phase: Nitrogen Collision Cross Sections Measured on a Prototype High Resolution Drift Tube Ion Mobility-Mass Spectrometer”, *Analytical Chemistry* 86, 2107-2116 (2014).

[2] Siems, WF; Wu, C; Tarver, EE; Hill Jr., HH; Larsen, PR; McMinn, DG; “Measuring the Resolving Power of Ion Mobility Spectrometers” *Analytical Chemistry* 66, 4195-4201 (1994).

[3] Revercomb, HE; Mason, EA; “Theory of Plasma Chromatography/Gaseous Electrophoresis— A Review” *Analytical Chemistry* 47(7), 970-983 (1975).